The dominant contribution of Southern Ocean heat uptake to time-evolving radiative feedback in CESM

Yuan-Jen Lin[1], Yen-Ting Hwang[1]†, Jian Lu[2], Fukai Liu[3], and Brian E. J. Rose[4]

[1]Department of Atmospheric Sciences, National Taiwan University, Taiwan

[2]Atmospheric Sciences and Global Change Division, Pacific Northwest National Laboratory, Richland, Washington, USA

[3]Key Laboratory of Physical Oceanography, Institute for Advanced Ocean Studies, Ocean University of China and Qingdao National Laboratory for Marine Science and Technology, Qingdao, China

[4]Department of Atmospheric and Environmental Sciences, University at Albany, State University of New York, Albany, New York, USA

†Corresponding author: Yen-Ting Hwang (ythwang@ntu.edu.tw)

Key Points:

- The increase in cloud feedback in CESM can be mostly attributed to the ocean heat uptake evolution in the Southern Ocean.
- The Southern Ocean heat uptake has a remote impact on the tropical surface temperature pattern, tropospheric stability, and cloud feedback.
- Models are consistent with the ocean heat uptake evolution in the Southern Ocean, although the magnitudes vary.

Abstract

Radiative feedbacks are found to vary with time in both historical records and future warming projections. Previous studies proposed two factors that determine the variation of radiative feedbacks: (i) the evolution of tropical sea surface warming patterns and (ii) the tropical-extratropical contrast of ocean heat uptake. Our results bridge the two factors by evaluating the remote impact from the extratropical ocean on tropical temperature patterns, accounting for the changes in radiative feedbacks. Based on the Green's Function approach that quantifies the non-local contributions of regional ocean heat uptake, we show that the net radiative feedback evolution in CESM can be mostly attributed to the heat uptake variations in the Southern Ocean. The enhanced surface warming associated with the weakened heat uptake decades after quadrupling CO_2 is not confined over the Southern Ocean, but extends to tropical Southeastern Pacific, which leads to decreasing tropospheric stability and more positive cloud feedbacks.

Plain Language Summary

Climate sensitivity, defined as surface temperature increase to doubling of carbon dioxide (CO_2) concentration, is a broadly used metric of anthropogenic climate change. However, it has spanned a wide range for decades due to the uncertainty in radiative forcing and feedback. The time evolution in radiative feedback, for example, adds challenges for evaluating climate sensitivity via simulations with limited length and for comparing model simulations with observational records. In this study, we investigate how the ocean influences the time evolution of radiative feedback. More specifically, we quantify the dependence of radiative feedback on regional ocean heat uptake in response to an abrupt increase in CO_2 concentration. Results show that the surface warming due to weakened ocean heat uptake over the Southern Ocean decades after CO_2 increase is not locally confined, but has far-field impacts on tropical clouds via remote influences on sea surface temperature and atmospheric stability in the tropics. The tropical sea surface temperature patterns have been shown to be key for understanding transient evolution of radiative feedbacks in previous studies; our findings further suggest that Southern Ocean heat uptake could be a potential root cause for these evolutions.

1 Introduction

Radiative feedbacks describe the efficiency by which the Earth system damps out radiative forcings such as increased greenhouse gases. Studies have long shown that the amplitudes of radiative feedbacks vary across models (Charney et al., 1979), largely accounting for the inter-model spread of global warming projections (Knutti et al., 2017). Recent studies have suggested that radiative feedbacks vary with time in historical and increasing CO_2 simulations, leading to challenges for predicting transient and equilibrium

climate sensitivities (Andrews et al., 2015; Gregory & Andrews, 2016). A mechanism named "pattern effect" is proposed to account for aspects of both the inter-model spread and the time dependence of radiative feedbacks (Stevens et al., 2016). Pattern effects refer to ways in which regional spatial patterns of sea surface temperature (SST) project onto radiative fluxes at the top-of-atmosphere (TOA), thus modulating the feedbacks. A detailed mechanistic understanding of pattern effects is an essential prerequisite for extrapolating future climate sensitivity from short-term transient observations.

Two somewhat different lines of argument have recently emerged. The tropical east-west SST gradient has been identified as a key factor influencing the radiative feedbacks via modification of the lower-tropospheric stability and low cloud cover (Ceppi & Gregory, 2019; Dong et al., 2019; Zhou et al., 2017). On the other hand, the spatial pattern of ocean heat uptake (OHU) has also been shown to have a strong effect on radiative feedbacks, with emphasis on the time-evolving relative magnitudes of tropical and extratropical OHU (Kang & Xie, 2014; Rose et al., 2014; Rose & Rayborn, 2016; Rugenstein et al., 2016). While the SST and OHU perspectives offer seemingly competing explanations for varying radiative feedbacks, some studies have linked the two perspectives by suggesting that the SST patterns on which the feedbacks depend are themselves driven non-locally by OHU patterns (Haugstad et al., 2017). However no study to date has provided a detailed quantitative attribution of the contribution of regional OHU to pattern effects and time-evolving feedbacks.

The goal of this study is to isolate the influence of ocean dynamics on the time-evolution of radiative feedbacks in response to an abrupt forcing (as represented by a fully coupled climate model). More specifically, we quantify the influence of time-evolving regional OHU on global SST patterns and radiative feedbacks. Our attribution is based on a linear systems approach: first, the time-dependent impact of ocean dynamics is determined through comparison of fully coupled and slab-ocean simulations; second, a Green's Function approach is used to attribute the local and far-field impacts of spatially localized OHU (F. Liu et al., 2018a). We first describe the simulations and linear attribution method (section 2). Results of our attribution (section 3) reveal the dominant role of OHU in the Southern Ocean on time-evolution of tropical SST patterns and radiative feedbacks. Similar OHU and radiative feedback evolution are found in most of the climate models participating in the Coupled Model Intercomparison Project Phase 5 (CMIP5).

2 Data and Method

2.1 Data

The transient responses of surface temperature (TS), estimated inversion strength (EIS; Wood and Bretherton (2006)), and radiative feedbacks are analyzed in both the fully coupled model CESM1 (CAM5.1, FV2; hereafter "FOM") and the atmospheric model CAM5 coupled

with a slab-ocean (hereafter "SOM"). Anomalies (denoted by "Δ") are calculated by subtracting the time-mean climatology under preindustrial conditions (piControl) from the transient, 150-year simulation forced by an abrupt quadrupling of CO_2 (abrupt4×CO_2). In piControl simulations, we substitute two particular variables (air temperature and relative humidity) in CESM1 (CAM5) for CESM1 (CAM5.1, FV2) due to the data availability. A 7-year low-pass Butterworth digital filter is applied to all the variables to remove the high-frequency variability. Also, we adopt 108 pairs of SOM simulations forced with ocean q-flux patches (F. Liu et al. (2018a); hereafter "SOM-Patches"; see Text S1) to construct a Green's Function (equation (3)), which indicates the dependence of climate responses on gridded OHU and can be used to evaluate the influences of OHU (section 2.2). Finally, we extend the analysis to 24 other CMIP5 models (Table S1).

2.2 Method

To isolate the ocean's role in affecting transient atmospheric and surface responses to CO_2 increase in the coupled climate system, we consider anomalous OHU due to including dynamical ocean as a forcing (i.e., heat sink/ source) to the atmosphere and surface, consistent with previous studies (Winton et al., 2010). In other words, as shown in equation (1), the transient atmospheric and surface responses to CO_2 increase in each grid cell i of FOM ($\Delta X_{i,\ FOM}$) can be partitioned into the same response in SOM ($\Delta X_{i,\ SOM}$) and the contribution from the anomalous OHU due to including a full dynamical ocean ($\Delta X_{i,\ dOHU}$), which is quantified via a Green's Function approach. X can be any of the atmospheric or surface variables such as TS, air temperature, or TOA radiative fluxes. By inferring TOA fluxes using the Green's Function, we treat the inferred fluxes as feedbacks to the original CO_2 forcing, though indirectly excited through the OHU. The residual (ε) accounts for the responses of X that are independent from OHU and the potential nonlinearities (Text S2).

$$\Delta X_{i,\ FOM} = \Delta X_{i,\ SOM} + \Delta X_{i,\ dOHU} + \varepsilon \quad (1).$$

To quantify $\Delta X_{i,\ dOHU}$, we calculate the difference in OHU between FOM and SOM in response to CO_2 increase ($dOHU$; equation (2); Figure S1), and evaluate its influences via the Green's Function matrix G (equation (3)), derived from weighting equilibrium responses of X in "SOM-patches" (consistent with Dong et al. (2019); Text S2).

$$dOHU_i = \Delta OHU_{i,\ FOM} - \Delta OHU_{i,\ SOM} \quad (2).$$

$$G = \begin{pmatrix} \frac{\partial X_1}{\partial OHU_1} & \cdots & \frac{\partial X_1}{\partial OHU_n} \\ \vdots & \ddots & \vdots \\ \frac{\partial X_n}{\partial OHU_1} & \cdots & \frac{\partial X_n}{\partial OHU_n} \end{pmatrix} \quad (3).$$

For any grid cell i, the response of atmospheric or surface variable X to large-scale $dOHU$ could be approximated by a first order Taylor series with respect to $dOHU$ at all grid

boxes j. Both i and j go from 1 to n, and n is the total number of grid points. We can thus quantify the non-local effects of $dOHU$ when grid i and j are apart.

$$\Delta X_{i,\ dOHU} = \sum_{j=1}^{n} \frac{\partial X_i}{\partial OHU_j} dOHU_j \quad (4).$$

By combining the equation (1) and (4), the atmospheric or surface responses in FOM can be reconstructed as follows:

$$\Delta X_{i,\ FOM} = \Delta X_{i,\ SOM} + \sum_{j=1}^{n} \frac{\partial X_i}{\partial OHU_j} dOHU_j + \varepsilon \ (5).$$

Since the ocean mixed layer depth at high latitudes is generally deeper in FOM than in SOM, and the ocean heat flux divergence evolves freely in FOM while is fixed in SOM, the transient difference in OHU between FOM and SOM ($dOHU$) is due to two processes. One is the anomalous OHU caused by deep ocean heat storage (which is absent in SOM), and the other is the anomalous OHU caused by changes in ocean heat flux divergence resulting from changes in oceanic circulation (e.g. due to wind-driven effects), or changes in oceanic temperature, or both. While the causes for evolving $dOHU$ are beyond the scope of the study, we discuss possible mechanisms driving the $dOHU$ evolution (section 4) and emphasize the influences of $dOHU$ on the evolution of radiative feedbacks (section 3).

3 Results

3.1 Linear reconstruction via Green's Function approach

Figures 1a and 1b demonstrate the responses of quadrupling CO_2 in FOM and SOM and the applicability of the Green's Function approach. While the initial TOA radiative forcing is similar between FOM and SOM in the abrupt4×CO_2 simulation, their time evolution of global-mean anomalous TS (ΔTS) and net TOA radiation (ΔR_{net}) in response to abrupt quadrupling of CO_2 is distinct. In the first 20 years, most of the radiative forcing is damped in the SOM, accompanied with strong TS increase of 8K. On the other hand, the radiative imbalance in FOM is still large and the increase in TS is about half of that in SOM. Results show that the contribution of $dOHU$, predicted by the Green's Function approach (section 2.2), mitigates surface warming by around 4K in the first two decades, and the cooling effect slowly weakens afterwards (blue line of Figure 1b). The contribution of $dOHU$ explains most of the difference in ΔTS and ΔR_{net} evolution between FOM and SOM (compare the black lines with gray lines in Figures 1a and 1b), indicating that the first-order linearity holds for the attribution system here. Similar linearity has been shown in the previous works (Boer & Yu, 2003; Marvel et al., 2016).

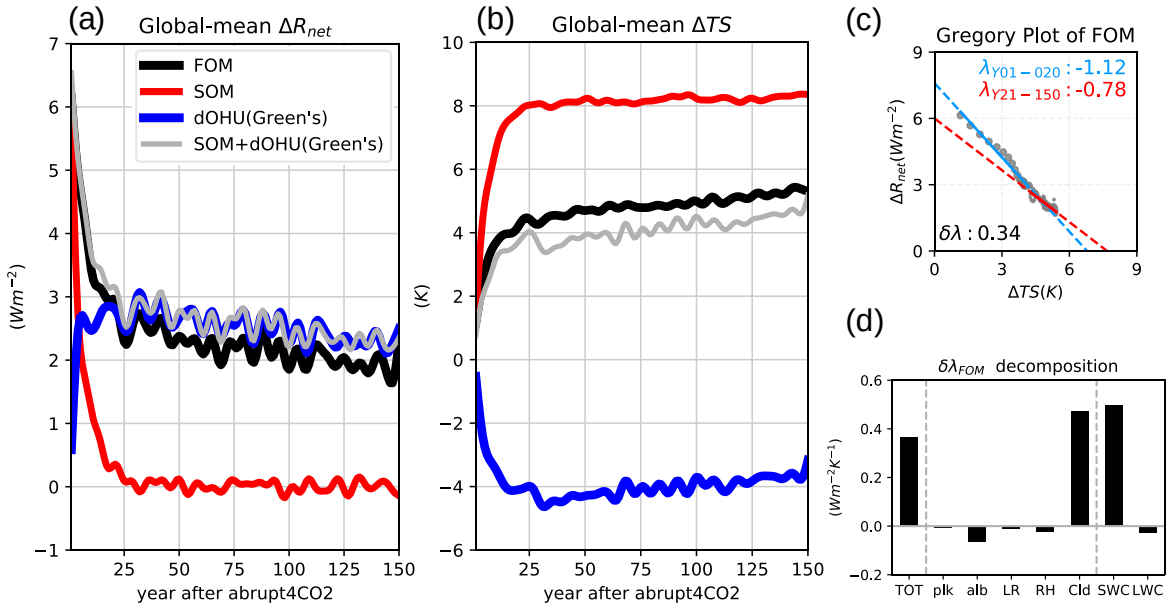

Figure 1. (a) Global-mean ΔR_{net} in FOM (black), and in SOM (red). The blue line shows ΔR_{net} evaluated from the Green's Function approach (equation (4)). The grey line shows the summation of the red and blue lines. (b) Same as (a), but for global-mean ΔTS. (c) Scatterplot of ΔR_{net} vs. ΔTS in FOM, following Gregory et al. (2004). (d) $\delta\lambda_{FOM}$ decomposition using radiative kernels method.

3.2 Attribute the radiative feedback evolution to regional OHU

Figure 1c illustrates the evolution of ΔR_{net} and ΔTS in the form of Gregory plot (Gregory et al., 2004). The radiative feedback parameter λ, calculated as the regression slope of ΔR_{net} against global-mean ΔTS, evolves from -1.12 $\frac{W}{m^2K}$ in year 1-20 to -0.78 $\frac{W}{m^2K}$ in year 21-150 in FOM. To quantify the transient increase of effective climate sensitivity, we define a feedback increment $\delta\lambda$ as

$$\delta\lambda_{FOM} = \frac{d\left(\overline{\Delta R_{net,\ FOM}}\right)}{d\left(\overline{\Delta TS_{FOM}}\right)}\bigg|_{Y21-150} - \frac{d\left(\overline{\Delta R_{net,\ FOM}}\right)}{d\left(\overline{\Delta TS_{FOM}}\right)}\bigg|_{Y1-20} \quad (6),$$

where overbars indicate global mean. The separation at year 20 approximately distinguishes between the fast and slow components of climate responses (Geoffroy et al., 2013; Held et al., 2010). The estimated $\delta\lambda$ for the FOM experiment here is 0.34 $\frac{W}{m^2K}$. Other CMIP5 models range from -0.18 to 1.04, with the multimodel mean of 0.51 (Andrews et al., 2015). To understand the time dependence of λ in FOM ($\delta\lambda_{FOM}$), we decompose ΔR_{net} into radiative anomalies that are related to changes in Planck emission (ΔR_{plk}), surface albedo (ΔR_{alb}),

lapse-rate (ΔR_{LR}), relative humidity (ΔR_{RH}), and clouds (ΔR_{Cld}) through radiative kernels method (Held & Shell, 2012; Soden et al., 2008), with the kernels calculated with CAM5 (Pendergrass et al., 2018):

$$\Delta R_{net} = \Delta R_{plk} + \Delta R_{alb} + \Delta R_{LR} + \Delta R_{RH} + \Delta R_{Cld} \quad (7).$$

Figure 1d shows that the increase in λ in FOM can be mostly attributed to the increase in net cloud feedback, especially the cloud's effect on the shortwave radiation, consistent with previous studies (Andrews et al., 2015; Ceppi & Gregory, 2017). To understand the cause of the cloud-induced radiative anomalies, we decompose it into two parts: one from SOM and the other excited by $dOHU$, based on the linearity of the climate system (as per equation (1) with $X = \Delta R_{Cld}$).

$$\Delta R_{Cld,\ FOM} = \Delta R_{Cld,\ SOM} + \Delta R_{Cld,\ dOHU} + \varepsilon \quad (8).$$

Also, the second term on the right hand side of equation (8) can be further decomposed into the changes excited by $dOHU$ from different regions by limiting the integration area of equation (4). Here we divide the global $dOHU$ into four latitude bands:

$$\Delta R_{Cld,\ dOHU} = \Delta R_{Cld,\ dOHU,\ 30N-90N} + \Delta R_{Cld,\ dOHU,\ EQ-30N} + \Delta R_{Cld,\ dOHU,\ EQ-30S} + \Delta R_{Cld,\ dOHU,\ 30S-90S} \quad (9).$$

Note that each radiative feedback contributes to part of the TOA flux variation by scaling with global-mean ΔTS, with the ΔTS the result of multiple simultaneous radiative feedbacks (Figure 2). Using changes in global-mean TS from the same reference system allows us to linearly decompose the net radiative feedback threefold, indicated by the three loops of Figure 2. In the first loop, the net radiative feedback is decomposed into the radiative feedbacks related to different physical processes (equation (7)). In the second loop, the net cloud feedback is decomposed into the contribution excluding and including the dynamical ocean, indicated by SOM data and the $dOHU$ contribution evaluated by the Green's Function approach, respectively (equation (8)). Similar decomposition can be done for other radiative feedbacks, though we focus here on cloud feedbacks due to their importance as revealed in Figure 1d. In the third loop, the contribution due to ocean dynamics is further decomposed into contributions due to $dOHU$ in four latitudes bands (equation (9)). This linear systems approach of attributing the changes in radiative feedbacks by decomposing radiative fluxes only instead of both radiative fluxes and TS has also been applied in previous studies (Roe, 2009; Rose & Rayborn, 2016).

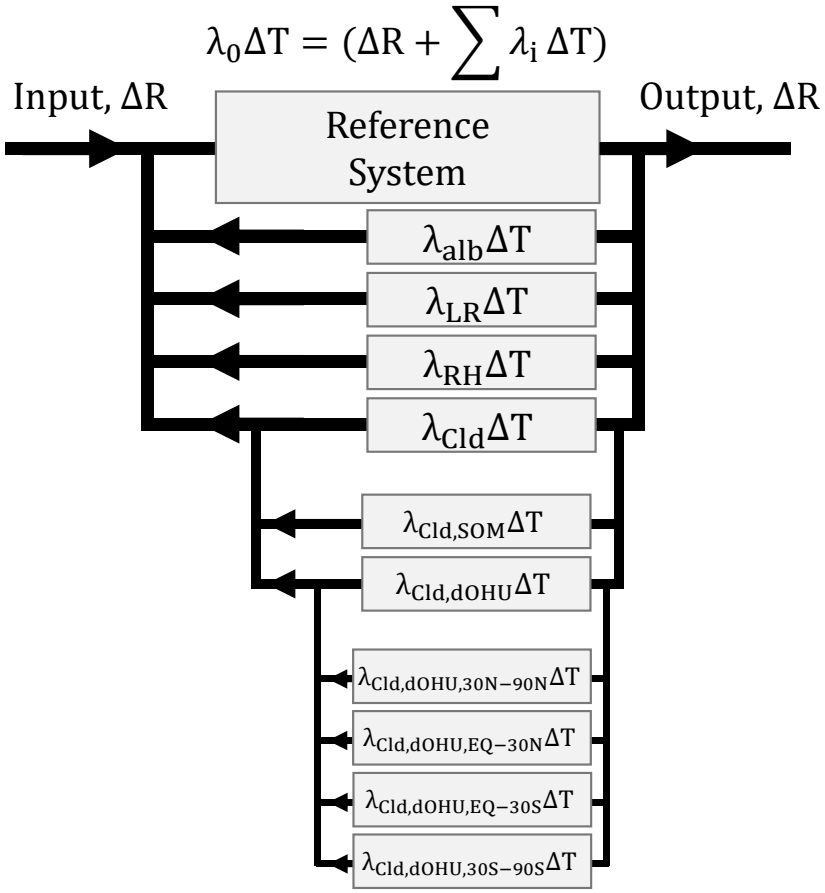

Figure 2. Schematic diagram of the decomposition of net radiative feedback, modified from Roe (2009).

The results of this decomposition are shown in Figures 3a-c. The shift toward more positive net cloud feedback in FOM ($\delta\lambda_{Cld,\ FOM}$; Figure 3b) arises predominantly from $dOHU$ in 30S-90S ($\delta\lambda_{Cld,\ dOHU,\ 30S-90S}$; Figure 3c), shown as the most positive bar in Figure 3a. Further analysis shows that 49% of the $\delta\lambda_{Cld,\ dOHU,\ 30S-90S}$ arises from tropical (30S-30N) cloud changes, implying a strong remote impact. Another 42% arises from local cloud changes in 30S-90S (Figure 3c). We describe the physical processes by which 30S-90S $dOHU$ result in increasingly positive local and remote cloud feedbacks as following three steps:

(a) Local and remote influence of $dOHU$ on SST: The $dOHU$ in 30S-90S (blue line of Figure 4a) strengthens throughout the first decade after quadrupling CO_2 but slowly decreases afterwards. When comparing early and late periods, the weakening tendency of $dOHU$ in the late period leads to the increasingly enhanced southern hemisphere (SH) warming. Importantly, the warming induced by the decreasing 30S-90S $dOHU$ is not confined to the Southern Ocean, but also extends to the subtropics via eastern basins (Figure 3f). This local and remote SH surface warming

pattern due to 30S-90S $dOHU$ is also found in FOM (albeit with weaker magnitude; Figure 3e), suggesting similar mechanisms operate in FOM. While the teleconnection mechanism needs further investigation, our findings are consistent with previous studies suggesting that extratropical OHU can affect tropical TS by modifying the trade winds strength associated with the anomalous cross-equatorial Hadley Cell (Hwang et al., 2017).

(b) Lower-tropospheric stability (LTS) determined by SST pattern: In both the Southern Ocean and the tropics, the evolution of LTS is influenced by δTS, but in different ways. Locally over the Southern Ocean, enhanced surface warming (positive δTS) destabilizes the lower troposphere (which we quantify through negative δEIS; Figures 3h and 3i). In tropics on the other hand, since tropospheric temperatures are strongly coupled to SST in the West Pacific (WP) convective regions according to the weak temperature gradient approximation (Sobel et al., 2002), LTS is largely determined by the surface warming contrast between convective and non-convective regions. We find that δTS in the Southeastern Pacific is more positive than in the WP convective region (gray box in Figures 3e and 3f), i.e. the East-West Pacific SST gradient is reduced, which explains the destabilization of the non-convective subtropical regions (Figures 3h and 3i). Significantly, we find consistent patterns of negative subtropical δEIS_{FOM} and $\delta EIS_{dOHU,30S-90S}$, strongly suggesting a causal but remote link between Southern Ocean heat uptake and tropical stability.

(c) Changes in cloud feedback linked to stability changes and other factors: The decrease in tropospheric stability acts to decrease the low cloud amount, since a weaker inversion is less efficient in trapping moisture in the boundary layer (Wood & Bretherton, 2006). The decrease in low cloud amount accounts for more positive cloud feedback by keeping more shortwave radiation in the climate system (Figures 3b and 3c).

In addition to the low cloud amount change discussed above, cloud albedo can also modify the strength of the cloud feedback. Area-weighted average of liquid water path (LWP) over 30S-90S increases by 30% in the first 20 years while local SST evolves from 276 to 279 K, causing phase changes in low-level clouds. In contrast, LWP holds nearly constant in the following 130 years while local SST is still rising. The halt of increasing LWP in the later periods results in a more positive shortwave cloud feedback (Figure S2), as the increase in LWP accounts for larger cloud albedo (McCoy et al., 2014; Zelinka et al., 2012). The LWP evolution in Southeastern Pacific also leads to more positive cloud feedback, while the cause for decreasing LWP might be related with the decrease in cloud amount (their time evolution is positively correlated with a coefficient of 0.71) as the local SST is too high for phase changes (Figure S2).

It is worth noting that the tropical δTS and δEIS in response to quadrupling CO_2 are

largely influenced remotely by Southern Ocean heat uptake, rather than local OHU evolution in tropics. Figure 3d quantifies the contribution of $dOHU$ over four different latitudinal bands on the tropical δTS by defining the evolution of WP index as the area-weighted averaged oceanic δTS in 50S-50N outside the WP minus that inside the WP. Results show that the increase in WP index in FOM is mostly due to the $dOHU$ evolution in 30S-90S. Consistently, the change in the S index, defined as area-weighted averaged 50S-50N oceanic δEIS (Ceppi & Gregory, 2017, 2019), can also be attributed to $dOHU$ in SH extratropics. The remote impact from extratropical OHU to tropical SST pattern bridges two hypotheses that both account for the changes in radiative feedbacks: one emphasizes the tropical east-west contrast of SST (Dong et al., 2019), and the other emphasizes the influence between tropical and extratropical OHU (Rose & Rayborn, 2016). Through its remote effects on tropical SST patterns and lower-tropospheric stability, heat uptake in the Southern Ocean can explain most of the change in net radiative feedback in FOM.

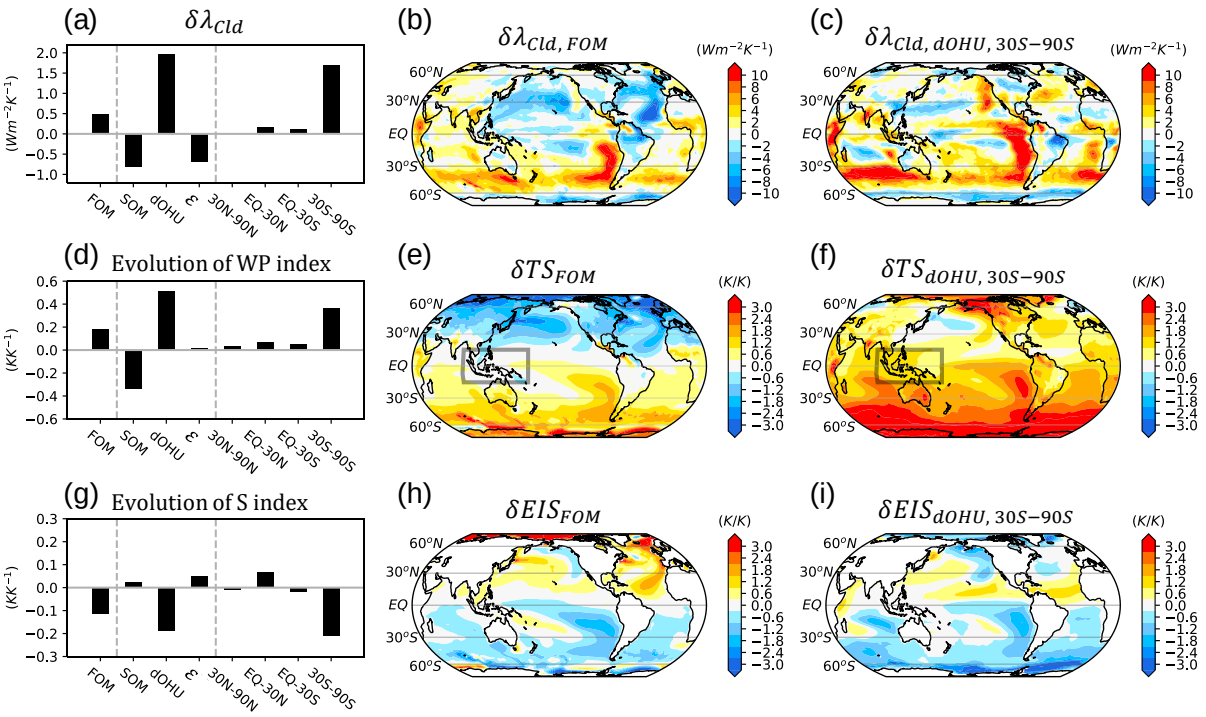

Figure 3. (a) The decomposition of $\delta\lambda_{Cld}$ (equation (7)-(9)). (b) $\delta\lambda_{Cld}$ pattern in FOM. (c) $\delta\lambda_{Cld}$ pattern due to $dOHU$ evolution over 30S-90S. (d) The decomposition of the evolution of WP index. Each is calculated as 50S-50N averaged oceanic δTS outside the WP minus that inside the WP. (e) δTS pattern in FOM. (f) δTS pattern due to $dOHU$ evolution over 30S-90S. (g) The decomposition of the evolution of S index. Each is calculated as 50S-50N averaged δEIS over ocean Ceppi and Gregory (2019). (h) δEIS pattern in FOM. (i) δEIS pattern due to $dOHU$ evolution over 30S-90S. The definition of δTS and δEIS

follow equation (6) but to replace radiative fluxes anomalies with TS and EIS anomalies, respectively.

3.3 CMIP5 models

In section 3.2, we conclude that $dOHU$ over Southern Ocean is the root cause of the increasingly positive net radiative feedback in FOM. Does this result hold for other models? Figure 4a shows that most of the CMIP5 models agree qualitatively on the $dOHU$ evolution over SH extratropics, which strengthens in the first decade after quadrupling CO_2 but slowly decreases afterwards. Though the amplitudes vary with models, the consistency of the SH extratropical $dOHU$ evolution suggests its local and remote impacts on SST and cloud feedback may be robust features among models. Consistent with our expectations, most CMIP5 models exhibit increasingly enhanced warming of the Southern Ocean and Southeastern Pacific, as well as decreased zonal tropical Pacific SST gradients (Figure 4c). The stronger warming over Southeastern Pacific relative to the WP leads to increase in net cloud feedback (Figure 4d) by decreasing the lower-tropospheric stability (not shown, consistent with Figure 1b of Ceppi and Gregory (2017)). While we cannot isolate the impacts of regional $dOHU$ on cloud feedback changes in individual CMIP5 model using the Green's function approach due to large residuals (Text S3), we emphasize the consistent SH extratropical $dOHU$ in CMIP5 models, and surmise it may be responsible for the increasingly enhanced warming, tropospheric stability, and net cloud feedback in the SH through the same causal mechanisms as we have demonstrated in our CESM simulations.

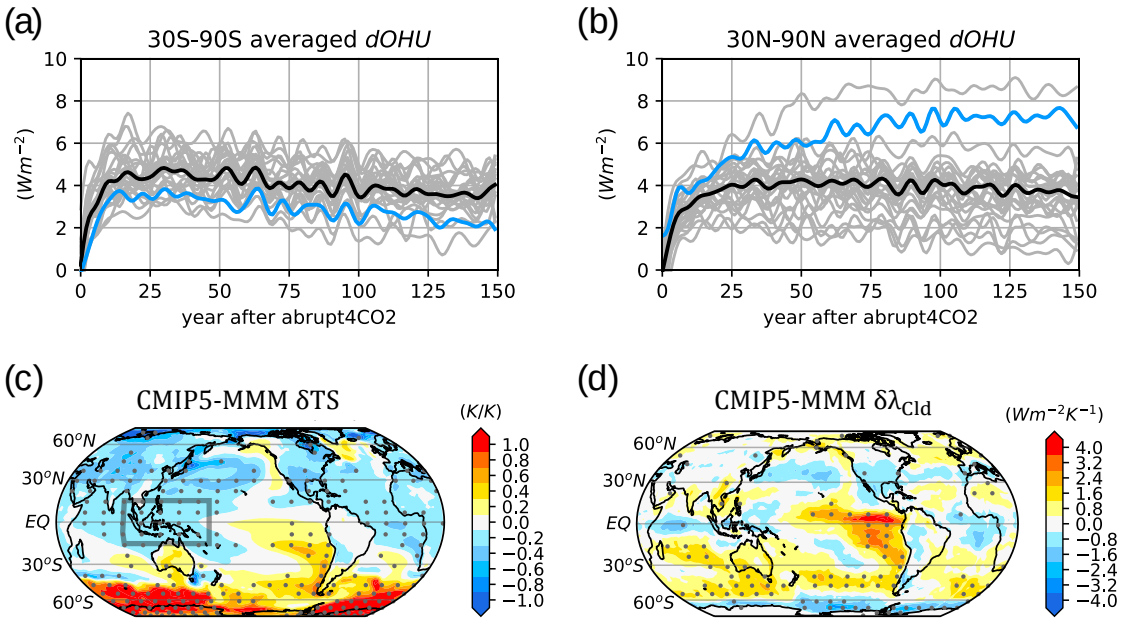

Figure 4. (a) 30S-90S averaged $dOHU$ ($\Delta OHU_{FOM} - \Delta OHU_{SOM}$) in each CMIP5 model (gray lines) and the model CESM (blue line). The black line indicates the CMIP5 multimodel mean. (b) The same as (a), but for 30N-90N averaged $dOHU$. Note that ΔOHU_{SOM} used here is the same across CMIP5 models (CAM5-SOM), while ΔOHU_{FOM} varies according to each model. (c) CMIP5 multimodel-mean δTS pattern. (d) CMIP5 multimodel-mean $\delta\lambda_{Cld}$ pattern. Dots indicate that the absolute value of the multimodel mean is larger than 0.5 standard deviation of the inter-model spread.

4 Summary and discussion

Cloud feedback has remained the primary source of model uncertainty in the global warming projection for decades (Soden & Held, 2006; Zelinka et al., 2017), with the subtropical low-level clouds contributing to most of the uncertainty (Bony & Dufresne, 2005; Myers & Norris, 2016). When focusing on observational records or the slow evolution of radiative feedbacks in abrupt4×CO_2 experiment, previous studies have quantified and demonstrated how tropical SST pattern influences subtropical low-level clouds (Andrews & Webb, 2018; Ceppi & Gregory, 2017; Gregory & Andrews, 2016; Zhou et al., 2016). Questions have remained about the ultimate causes of the time-evolution of these radiatively-important tropical SST patterns.

In this work we used a Green's Function approach to perform a detailed non-local linear attribution of the time-evolution of cloud feedbacks and SST patterns to regional ocean dynamics in response to abrupt4×CO_2 forcing. Through this approach (which relies on comparisons between fully coupled and slab ocean models) we have shown that the evolving tropical SST pattern is driven remotely by variations in Southern Ocean heat uptake. This effect is most prominent in the Southeast subtropical Pacific, where the increasingly enhanced warming is driven by slowly weakening Southern Ocean heat uptake, and leads to low-cloud loss and a more positive net cloud feedback. Rose et al. (2014) and Rugenstein et al. (2016) have suggested OHU being the root cause of evolution of radiative feedbacks. Here, we further highlight the critical role of the Southern Ocean, which is likely to be the root cause of the evolution of tropical SST patterns and cloud radiative feedbacks in abrupt4×CO_2 simulation in FOM.

While CMIP5 models generally agree on the rapid increase and then slow decline of Southern Ocean heat uptake, their magnitudes vary. An implication of the remote influence demonstrated in this study is that uncertainty in the evolution of subtropical low-level clouds and cloud feedbacks could be partly traced to uncertainty in the evolution of Southern Ocean heat uptake, as suggested by Rose and Rayborn (2016). In addition, there exists a large inter-model spread in the evolution of OHU over Northern Hemisphere (NH) extratropics (Figure 4b). The NH surface temperature and cloud feedback evolution also appear to be less

robust among models (Figures 4c and 4d). In contrary to OHU over Southern Ocean that is mostly determined by the mean state of the ocean (Armour et al., 2016; W. Liu et al., 2018; Manabe et al., 1990; Marshall et al., 2014), one of the key factors determining OHU in the NH is the variations of Atlantic Meridional Overturning Circulation (AMOC; Chen and Tung (2018); Kostov et al. (2014)). The time evolution of AMOC intensity, including the weakening within decades after increasing CO_2 and the re-strengthening in timescales of hundreds of years (Cheng et al., 2013; Stouffer et al., 2006), have been shown to modulate radiative feedbacks (Caesar et al., 2020; Lin et al., 2019; Trossman et al., 2016). Focusing on a single model (CESM), our work highlights the critical role of the Southern Ocean. For inter-model spread or for models with more apparent AMOC re-strengthening, OHU over Southern Ocean and North Atlantic could both be important for the transient increase of effective climate sensitivity. We suggest the base climate oceanic circulation may thus have an important influence on climate sensitivity via affecting the evolution of ocean heat uptake, which then alters cloud radiative effects both locally and remotely.

Acknowledgments

We acknowledge the World Climate Research Program's Working Group on Coupled Modelling, which is responsible for CMIP, and we thank the climate modeling groups (Table S1) for producing and making available their model output. For CMIP the U.S. Department of Energy's Program for Climate Model Diagnosis and Intercomparison provided coordinating support and led development of software infrastructure in partnership with the Global Organization for Earth System Science Portals. All CMIP data can be downloaded from the ESGF at https://esgf-node.llnl.gov/projects/esgf-llnl/. This research was undertaken with the assistance of resources and services from the National Energy Research Scientific Computing Center (NERSC), supported by the U.S. Government. Processed data to support the analysis is published with doi: 10.5281/zenodo.3987888.

YJL and YTH were supported by Ministry of Science and Technology of Taiwan (MOST 109-2636-M-002-011-). JL was supported by the U.S. Department of Energy Office of Science Biological and Environmental Research as part of the Regional and Global Modeling and Analysis program. FL was supported by the National Natural Science Foundation of China (NSFC; 41906002 and 91858210). BEJR was supported by NSF grant AGS-1455071.

References

Andrews, T., Gregory, J. M., & Webb, M. J. (2015). The Dependence of Radiative Forcing and Feedback on Evolving Patterns of Surface Temperature Change in Climate Models. *Journal of Climate*, *28*(4), 1630-1648. doi:10.1175/Jcli-D-14-00545.1

Andrews, T., & Webb, M. J. (2018). The Dependence of Global Cloud and Lapse Rate Feedbacks on the Spatial Structure of Tropical Pacific Warming. *Journal of Climate*, *31*(2), 641-654.

Armour, K. C., Marshall, J., Scott, J. R., Donohoe, A., & Newsom, E. R. (2016). Southern Ocean warming delayed by circumpolar upwelling and equatorward transport. *Nature Geoscience*, *9*(7), 549-+. doi:10.1038/ngeo2731

Boer, G., & Yu, B. (2003). Climate sensitivity and response. *Climate Dynamics*, *20*(4), 415-429.

Bony, S., & Dufresne, J. L. (2005). Marine boundary layer clouds at the heart of tropical cloud feedback uncertainties in climate models. *Geophysical Research Letters*, *32*(20).

Caesar, L., Rahmstorf, S., & Feulner, G. (2020). On the relationship between Atlantic meridional overturning circulation slowdown and global surface warming. *Environmental Research Letters*, *15*(2), 024003.

Ceppi, P., & Gregory, J. M. (2017). Relationship of tropospheric stability to climate sensitivity and Earth's observed radiation budget. *Proceedings of the National Academy of Sciences*. doi:10.1073/pnas.1714308114

Ceppi, P., & Gregory, J. M. (2019). A refined model for the Earth's global energy balance. *Climate Dynamics*. doi:10.1007/s00382-019-04825-x

Charney, J. G., Arakawa, A., Baker, D. J., Bolin, B., Dickinson, R. E., Goody, R. M., . . . Wunsch, C. I. (1979). *Carbon dioxide and climate: a scientific assessment*: National Academy of Sciences, Washington, DC.

Chen, X., & Tung, K.-K. (2018). Global surface warming enhanced by weak Atlantic overturning circulation. *Nature*, *559*(7714), 387-391.

Cheng, W., Chiang, J. C., & Zhang, D. (2013). Atlantic meridional overturning circulation (AMOC) in CMIP5 models: RCP and historical simulations. *Journal of Climate*, *26*(18), 7187-7197.

Dong, Y., Proistosescu, C., Armour, K. C., & Battisti, D. S. (2019). Attributing Historical and Future Evolution of Radiative Feedbacks to Regional Warming Patterns using a Green's Function Approach: The Preeminence of the Western Pacific. *Journal of Climate*(2019).

Geoffroy, O., Saint-Martin, D., Bellon, G., Voldoire, A., Olivié, D., & Tytéca, S. (2013). Transient climate response in a two-layer energy-balance model. Part II: Representation of the efficacy of deep-ocean heat uptake and validation for CMIP5

AOGCMs. *Journal of Climate, 26*(6), 1859-1876.

Gregory, J., Ingram, W., Palmer, M., Jones, G., Stott, P., Thorpe, R., . . . Williams, K. (2004). A new method for diagnosing radiative forcing and climate sensitivity. *Geophysical Research Letters, 31*(3).

Gregory, J. M., & Andrews, T. (2016). Variation in climate sensitivity and feedback parameters during the historical period. *43*(8), 3911-3920. doi:10.1002/2016gl068406

Haugstad, A., Armour, K., Battisti, D., & Rose, B. (2017). Relative roles of surface temperature and climate forcing patterns in the inconstancy of radiative feedbacks. *Geophysical Research Letters, 44*(14), 7455-7463.

Held, I. M., & Shell, K. M. (2012). Using Relative Humidity as a State Variable in Climate Feedback Analysis. *Journal of Climate, 25*(8), 2578-2582. doi:10.1175/Jcli-D-11-00721.1

Held, I. M., Winton, M., Takahashi, K., Delworth, T., Zeng, F., & Vallis, G. K. (2010). Probing the fast and slow components of global warming by returning abruptly to preindustrial forcing. *Journal of Climate, 23*(9), 2418-2427.

Hwang, Y. T., Xie, S. P., Deser, C., & Kang, S. M. (2017). Connecting tropical climate change with Southern Ocean heat uptake. *Geophysical Research Letters, 44*(18), 9449-9457.

Kang, S. M., & Xie, S.-P. (2014). Dependence of climate response on meridional structure of external thermal forcing. *Journal of Climate, 27*(14), 5593-5600.

Knutti, R., Rugenstein, M. A. A., & Hegerl, G. C. (2017). Beyond equilibrium climate sensitivity. *Nature Geosci, 10*(10), 727-736. doi:10.1038/ngeo3017

http://www.nature.com/ngeo/journal/v10/n10/abs/ngeo3017.html#supplementary-information

Kostov, Y., Armour, K. C., & Marshall, J. (2014). Impact of the Atlantic meridional overturning circulation on ocean heat storage and transient climate change. *Geophysical Research Letters, 41*(6), 2108-2116.

Lin, Y. J., Hwang, Y. T., Ceppi, P., & Gregory, J. M. (2019). Uncertainty in the evolution of climate feedback traced to the strength of the Atlantic Meridional Overturning Circulation. *Geophysical Research Letters, 46*(21), 12331-12339.

Liu, F., Lu, J., Garuba, O., Leung, L. R., Luo, Y., & Wan, X. (2018a). Sensitivity of Surface Temperature to Oceanic Forcing via q-Flux Green's Function Experiments. Part I: Linear Response Function. *Journal of Climate, 31*(9), 3625-3641.

Liu, F., Lu, J., Garuba, O. A., Huang, Y., Leung, L. R., Harrop, B. E., & Luo, Y. (2018b). Sensitivity of surface temperature to oceanic forcing via q-flux Green's function experiments Part II: Feedback decomposition and polar amplification. *Journal of Climate*(2018).

Liu, W., Lu, J., Xie, S.-P., & Fedorov, A. (2018). Southern Ocean heat uptake, redistribution, and storage in a warming climate: The role of meridional overturning circulation.

Journal of Climate, 31(12), 4727-4743.

Manabe, S., Bryan, K., & Spelman, M. J. (1990). Transient response of a global ocean-atmosphere model to a doubling of atmospheric carbon dioxide. *Journal of Physical Oceanography, 20*(5), 722-749.

Marshall, J., Armour, K. C., Scott, J. R., Kostov, Y., Hausmann, U., Ferreira, D., . . . Bitz, C. M. (2014). The ocean's role in polar climate change: asymmetric Arctic and Antarctic responses to greenhouse gas and ozone forcing. *Philos Trans A Math Phys Eng Sci, 372*(2019), 20130040. doi:10.1098/rsta.2013.0040

Marvel, K., Schmidt, G. A., Miller, R. L., & Nazarenko, L. S. (2016). Implications for climate sensitivity from the response to individual forcings. *Nature Climate Change, 6*(4), 386-389.

McCoy, D. T., Hartmann, D. L., & Grosvenor, D. P. (2014). Observed Southern Ocean cloud properties and shortwave reflection. Part II: Phase changes and low cloud feedback. *Journal of Climate, 27*(23), 8858-8868.

Myers, T. A., & Norris, J. R. (2016). Reducing the uncertainty in subtropical cloud feedback. *Geophysical Research Letters, 43*(5), 2144-2148.

Pendergrass, A. G., Conley, A., & Vitt, F. M. (2018). Surface and top-of-atmosphere radiative feedback kernels for CESM-CAM5. *Earth System Science Data, 10*(1), 317-324.

Roe, G. (2009). Feedbacks, timescales, and seeing red. *Annual Review of Earth and Planetary Sciences, 37*, 93-115.

Rose, B. E. J., Armour, K. C., Battisti, D. S., Feldl, N., & Koll, D. D. B. (2014). The dependence of transient climate sensitivity and radiative feedbacks on the spatial pattern of ocean heat uptake. *Geophysical Research Letters, 41*(3), 1071-1078. doi:10.1002/2013gl058955

Rose, B. E. J., & Rayborn, L. (2016). The Effects of Ocean Heat Uptake on Transient Climate Sensitivity. *Current Climate Change Reports, 2*(4), 190-201. doi:10.1007/s40641-016-0048-4

Rugenstein, M. A. A., Caldeira, K., & Knutti, R. (2016). Dependence of global radiative feedbacks on evolving patterns of surface heat fluxes. *Geophysical Research Letters, 43*(18), 9877-9885. doi:10.1002/2016gl070907

Sobel, A. H., Held, I. M., & Bretherton, C. S. (2002). The ENSO signal in tropical tropospheric temperature. *Journal of Climate, 15*(18), 2702-2706.

Soden, B. J., & Held, I. M. (2006). An assessment of climate feedbacks in coupled ocean–atmosphere models. *Journal of Climate, 19*(14), 3354-3360.

Soden, B. J., Held, I. M., Colman, R., Shell, K. M., Kiehl, J. T., & Shields, C. A. (2008). Quantifying climate feedbacks using radiative kernels. *Journal of Climate, 21*(14), 3504-3520.

Stevens, B., Sherwood, S. C., Bony, S., & Webb, M. J. (2016). Prospects for narrowing

484 bounds on Earth's equilibrium climate sensitivity. *4*(11), 512-522.
485 doi:10.1002/2016ef000376
486 Stouffer, R. J., Yin, J., Gregory, J., Dixon, K., Spelman, M., Hurlin, W., . . . Hasumi, H.
487 (2006). Investigating the causes of the response of the thermohaline circulation to past
488 and future climate changes. *Journal of Climate, 19*(8), 1365-1387.
489 Taylor, K., Crucifix, M., Braconnot, P., Hewitt, C., Doutriaux, C., Broccoli, A., . . . Webb, M.
490 (2007). Estimating shortwave radiative forcing and response in climate models.
491 *Journal of Climate, 20*(11), 2530-2543.
492 Trossman, D., Palter, J., Merlis, T., Huang, Y., & Xia, Y. (2016). Large-scale ocean
493 circulation-cloud interactions reduce the pace of transient climate change.
494 *Geophysical Research Letters, 43*(8), 3935-3943.
495 Vial, J., Dufresne, J.-L., & Bony, S. (2013). On the interpretation of inter-model spread in
496 CMIP5 climate sensitivity estimates. *Climate Dynamics, 41*(11-12), 3339-3362.
497 Webb, M. J., Lock, A. P., Bretherton, C. S., Bony, S., Cole, J. N., Idelkadi, A., . . . Ogura, T.
498 (2015). The impact of parametrized convection on cloud feedback. *Philosophical*
499 *Transactions of the Royal Society A: Mathematical, Physical and Engineering*
500 *Sciences, 373*(2054), 20140414.
501 Winton, M., Takahashi, K., & Held, I. M. (2010). Importance of Ocean Heat Uptake Efficacy
502 to Transient Climate Change. *Journal of Climate, 23*(9), 2333-2344.
503 doi:10.1175/2009jcli3139.1
504 Wood, R., & Bretherton, C. S. (2006). On the relationship between stratiform low cloud cover
505 and lower-tropospheric stability. *Journal of Climate, 19*(24), 6425-6432.
506 Zelinka, M. D., Klein, S. A., & Hartmann, D. L. (2012). Computing and partitioning cloud
507 feedbacks using cloud property histograms. Part II: Attribution to changes in cloud
508 amount, altitude, and optical depth. *Journal of Climate, 25*(11), 3736-3754.
509 Zelinka, M. D., Randall, D. A., Webb, M. J., & Klein, S. A. (2017). Clearing clouds of
510 uncertainty. *Nature Climate Change, 7*(10), 674-678.
511 Zhou, C., Zelinka, M. D., & Klein, S. A. (2016). Impact of decadal cloud variations on the
512 Earth’s energy budget. *Nature Geoscience, 9*(12), 871.
513 Zhou, C., Zelinka, M. D., & Klein, S. A. (2017). Analyzing the dependence of global cloud
514 feedback on the spatial pattern of sea surface temperature change with a Green's
515 function approach. *Journal of Advances in Modeling Earth Systems, 9*(5), 2174-2189.
516